Active Interaction Control Applied to a Lower Limb Rehabilitation Robot by Using EMG Recognition and Impedance Model

Wei Meng[1,2], Quan Liu[1,2], Zude Zhou[1,2], Qingsong Ai[1,2 *]

[1] Key Laboratory of Fiber Optic Sensing Technology and Information Processing, Ministry of Education

[2] School of Information Engineering, Wuhan University of Technology

Wuhan, Hubei 430070, China

* Corresponding author: qingsongai@whut.edu.cn

Abstract:

Purpose: The purpose is to propose a seamless active interaction control method integrating the electromyography (EMG)-triggered assistance and the adaptive impedance control scheme for parallel robot-assisted lower limb rehabilitation and training.

Design/methodology/approach: An active interaction control strategy based on EMG motion recognition and adaptive impedance model is implemented on a six-DOF parallel robot for lower limb rehabilitation. The autoregressive (AR) coefficients of EMG signals integrating with a support vector machine (SVM) classifier are utilized to predict the movement intention and trigger the robot assistance. An adaptive impedance controller is adopted to influence the robot velocity during the exercise, and in the meantime the user's muscle activity level is online evaluated and the robot impedance is adapted in accordance with recovery conditions.

Findings: Experiments on healthy subjects demonstrated that the proposed method was able to drive the robot according to the user's intention and the robot impedance can be updated with the muscle conditions. Within the movement sessions, there was a distinct increase in the muscle activity levels for all subjects with the active mode in comparison to the EMG-triggered mode.

Originality/value: Both users' movement intention and voluntary participation are considered, not only triggering the robot when people attempt to move, but also changing the robot movement in accordance with user's efforts. The impedance model here responds directly to velocity changes, and thus allows the exercise along a physiological trajectory. Moreover, the muscle activity level depends on both the normalized EMG signals and the weight coefficients of involved muscles.

Keywords: rehabilitation robot; EMG signals; motion recognition; muscle activity level; adaptive impedance control

1. Brief Introduction

According to the official statistical data from the United Nations, the proportion of the world's population over 60 years old will be doubled from 11% to 22% between year 2000 and 2050. Meanwhile, there are about 650 million disabled people worldwide, accounting for around 10% of the total world population. Currently, there is a considerable increase in the needs of health care and rehabilitation, especially among elderly or disabled people (Zhou *et al.*, 2013). Rehabilitation and medical robotics can not only liberate the therapists from heavy training missions, but also help the patients perform scientific and repetitive training to provide a better motor function recovery. Since electromyography (EMG) signals contain much information of the muscle activity and can imply people's movement action 30~100ms in advance (Fan and Yin, 2013), they are widely used in clinical diagnosis, rehabilitation, prosthetic control, and human-robot interaction. Benitez *et al.* (2013) gave an overview of different forms of therapy, and explained the benefits of

robotic aided rehabilitation by monitoring and analyzing the bio-signals from patient. Krebs *et al.* (2003) described a concept of performance-based progressive robot therapy that utilized EMG thresholds to initiate the robot assistance. In the research, the EMG signals in fourteen muscles of the upper limb were collected, and the assistance was triggered when the muscles' activity increased above a threshold. This EMG-triggered assistance encourages self initiated movement by patients, and this means the patient has to apply some voluntary efforts to obtain a movement supported by the robot. However, this approach usually breaks the movement into two separate phases, an active phase driven by the patient, and a passive phase driven by the robot (Marchal-Crespo and Reinkensmeyer, 2009). Furthermore, when the robot is driven to provide assistance in the second phase, typically passive controllers will be used to achieve the necessary movement, so the patient is not in a fully compliant environment when assistance is provided (Wolbrecht *et al.*, 2008). In such EMG-triggered mode, the robot would operate with a predefined trajectory after being activated, which had no interaction with the human limbs during this period until the time allowed for the next trigger event (Song *et al.*, 2008).

To increase patient's interactivity during the rehabilitation, the patient-cooperative strategy should be combined with approaches that adapt the robot assistance according to the intention of subjects. DiCicco *et al.* (2004) presented an orthotic exoskeleton controlled by EMG signals with threshold approach, which means the robot can be only activated when the normalized EMG signals are above a certain threshold. However, as explained above, this method may divide the robot assistance into two independent sub-tasks. Therefore, the self-initiated movement support and patient-cooperative control strategies must be integrated into a robot-assisted rehabilitation system. Benitez *et al.* (2013) proposed a set of dynamic models to compute the robot triggering function and the assistance level people needed by using the muscular EMG signals and the sensor information from robot. The models can be integrated into an active 1-DOF-elbow orthosis system, which provides a promising solution to such active rehabilitation problems. On the other hand, Song *et al*. (2013) proposed a continuous robot assistance method to provide robot assistive torque proportional to the amplitude of EMG signals. However, the relationship between EMG and joint torque was only simplified as a linear model. Many researchers utilized EMG signals to estimate the joint torque, and applied the estimated torque to the robot-assisted movement. Lenzi *et al*. (2012) studied a torque estimation-based EMG control method for powered exoskeletons, and the assistance was provided through a proportional EMG controller. These methods could provide effective support to the user. However, their usability was strongly limited by the application environment and the estimation of user muscular torque was quite rough. The development of pattern classification can help patients perform rehabilitation with EMG controlled robotic system. A human-assisting manipulator operated by EMG signals and arm motions was proposed by Fukuda *et al*. (2003), where an active joint in the manipulator's end-effector was controlled based on EMG pattern discrimination. So, the robot can adapt itself to the changes of EMG patterns according to the differences among individuals. Similarly, Kiguchi and Hayashi (2012) proposed an EMG-based method to control an upper-limb robot according to user's intention, in which, however, sixteen channels of EMG signals were captured to estimate the upper-limb joint torque vector. To have a better recognition accuracy, Ju *et al*. (2013) investigated nonlinear EMG features and classifiers, which made the robot system more reliable (Ouyang *et al*., 2014).

The potential problem with EMG-triggered passive robot training is that it does not consider patient's voluntary participation or muscular efforts, thus reducing the capabilities of the system to

exercise (Riener *et al*., 2006). The patient's muscle activity level can be reflected by EMG signals, while the voluntary participation is closely related to the interaction force between the patient and the robot. Several control strategies have been developed to provide robotic assistance according to the patient's disability level and the patient's voluntary participation in the training process. In most literatures, the subject's muscle activation level is evaluated by using root mean square (RMS) of EMG signals collected from related muscles. However, the level of EMG readings is dependent on the skin impedance at the electrodes location, which may vary between different sessions (Mobasser *et al*., 2007). So in order to compensate this variability, the EMG data have to be normalized. Song *et al*. (2008) used the maximum voluntary contraction (MVC) method to normalize EMG signals. In fact, using this method to calculate the muscle activity level is problematic as there will be very different contributions of each muscle when conducting different motion patterns (Ji and Liu, 2010). Thus, the weights of constriction muscles of the limb have to be reconsidered when evaluating patient's muscular strength. On the other hand, the human robot interaction control is mostly achieved by the use of impedance control. It is widely accepted that the behavior of robot should be adjusted according to patient's recovery conditions, which can be reflected from muscle activities (Ai *et al.*, 2014). The basis of adaptive impedance assistance is to modify the robot motion in a way that is desired by the patient, which is believed to be most appropriate for rehabilitation. However, the issue of reference trajectory adaptation has some drawbacks, for example, the extent of trajectory adaptation can not be well determined and the changes may result in an un-physiological motion pattern. In order to tackle this problem, the robot assistance speed can be adaptable (Duchaine *et al*., 2007). In this situation, the physiological trajectory can be followed, while the change in the motion velocity influenced by the patient can also be obtained in the meantime. Therefore, it may provide a better opportunity for the patient to actively contribute muscular efforts during the exercise compared to trajectory control.

Interactive rehabilitation and training encourages patient's active participation and may aid in rapid motor function recovery (Liu, 2011). In this paper, an active interaction controller is built by the fusion of EMG signals (reflecting human movement intention) and the force sensor (providing human-robot interaction information). In order to obtain the surface EMG signals from lower limb muscles more conveniently and effectively, a wireless EMG acquisition device based on Wi-Fi protocol is developed. An effective motion recognition controller based on autoregressive (AR) features and support vector machine (SVM) classifier is established to predict lower limb motion intention in advance and trigger the robot assistance. In order to allow the user to interact with the robot and take more efforts during the rehabilitation, an impedance controller is designed to make the robot movement speed adaptable to people's participation efforts. Furthermore, the impedance controller takes into account the user's muscle activity levels, which are evaluated from EMG signals by considering the contributions of each muscle in different motion patterns, to adapt the robot compliance accordingly. The proposed active interaction controller allows the patients to determine the trajectory pattern by recognizing EMG signals and influence the speed of their leg movements along a physiological trajectory during the whole practice.

2. A Lower Limb Rehabilitation Robot

The mechanical design of the robot is the basis of robot-assisted rehabilitation system. In general, there are two types of rehabilitation robots: end-effector robots, and exoskeleton-type robots. The exoskeleton robots usually have to be worn by the patient, and such robots have drawbacks of

inferior adaptability to different patients. On the contrary, the end-effector robots usually contact with the patient body at a certain point, making this type of robot easy to design and control. Although a number of robots show great prospect in the rehabilitation of the lower limbs, they have not yet been widely applied to the clinical rehabilitation (Yin *et al*., 2012). In order to avoid complex dynamics problems such as coupling effects caused by multi-DOFs, the human-machine interface in (Yin *et al*., 2012) was applied to the knee controlling with only one DOF joint extension. However, this structure can not meet the requirement of lower limb movement in multi-DOFs. Recently, parallel robots have drawn a lot of interests in the robotic community due to their superiority over the classical serial structures in terms of stiffness, accuracy, and high payload. It has been found that parallel robots are better candidates for lower limb rehabilitation (Jamwal *et al*., 2014). Hussain *et al*. (2011) had also proposed a 4-axis redundant parallel robot based on the modeling and kinematics of ankle anatomy.

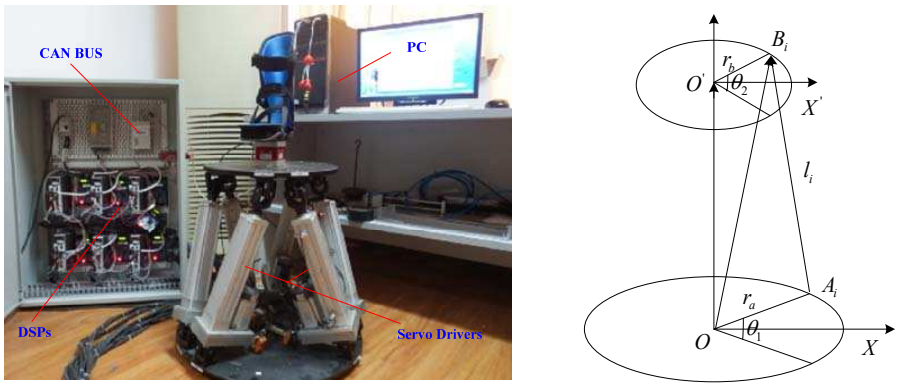

(a) the parallel robot and its control system *(b) the geometric diagram*

Figure 1 *A 6-DOF parallel robot for lower limb rehabilitation.*

The lower limb rehabilitation robot designed here is also basically a parallel mechanism with six transitional and rotational DOFs. The mechanical structure is composed of a fixed base, a moving platform, and six actuated limbs with kinematic chains. The Stewart platform shown in Figure 1 was designed by the authors' research group for the purpose of investigating lower limb rehabilitation. The designed robot can be adaptable to subjects of varying lower-limb abilities. Specifically, the system mainly includes an industrial PC, six motion controllers based on DSPs (model: TMS320LF2407A), Panasonic Minas servo drivers, as well as the Stewart platform. Linear position and velocity of each actuator are measured by incremental photoelectric encoders. The controller is coded in C++ language and runs under a Windows environment. The device is interfaced to a standard PC through a CAN BUS interface. Geometric diagram of the Stewart platform can be seen in Figure 1(b), where the radius of the upper platform is defined as r_b, and the angle is θ_2, likewise, the parameters of the fixed platform are defined as r_a and θ_1, respectively. The radius of the upper moving plate is 180*mm*, while the radius of the fixed base plate is 270*mm*, and the angles of the platforms are 28°and 22°, respectively. The robot's range of motion is able to fully meet the requirements of lower limb rehabilitation and training.

3. Wireless EMG Acquisition Device Based on Wi-Fi Protocol

It is important for the assistive rehabilitation robot to be controlled in accordance with the user's motion intention, which can be directly reflected by the biological signals. However, it is difficult to combine the biofeedback with the mechanical robot control (Riener *et al*., 2005), since the

traditional EMG acquisition devices are always wired, inconvenient, and non-portable. The current wireless techniques for EMG equipment usually focus on Bluetooth, Zigbee, or FSK (Hussain *et al*., 2013). The disadvantage is that the collected EMG data can only be used for local processing. As the Wi-Fi protocol has advantages of network access ability, high transmission bandwidth and low error rate over other wireless techniques, it can be used to complete the wireless transmission of EMG signals from the acquisition devices to the processing platforms. There are several commercial Wi-Fi based EMG acquisition devices, such as the BTS FREEEMG from BTS Bioengineering Corp. and the devices from Shanghai NCC Medical Co., Ltd. However, these commercial equipments are not selected by the authors because they are very expensive and this will increase the cost dramatically. The real-time performance is indeed an important issue when applying EMG devices to robot control. The self-developed device can also satisfy the real-time requirement by using Wi-Fi protocol. Considering the system compatibility when integrating it with the robot platform in our experiment, we choose to develop such a device by ourselves. The wireless EMG acquisition device designed by the researcher's group is presented in Figure 2, in which (a) is the system architecture, and (b) is the picture of the hardware device. The central unit is a high-performance monolithic processor STM32F103RC6, and the communication unit employs a WM-MR-08 module as the 802.11b/g baseband controller. In addition, the device is also integrated within a lithium battery and a power management system. Specifically, the sampling resolution is 12bit, with a bandwidth of 20~500Hz. The system amplification gain is set to 60db, wherein the preamplifier gain is 20db and the final gain is 40db.

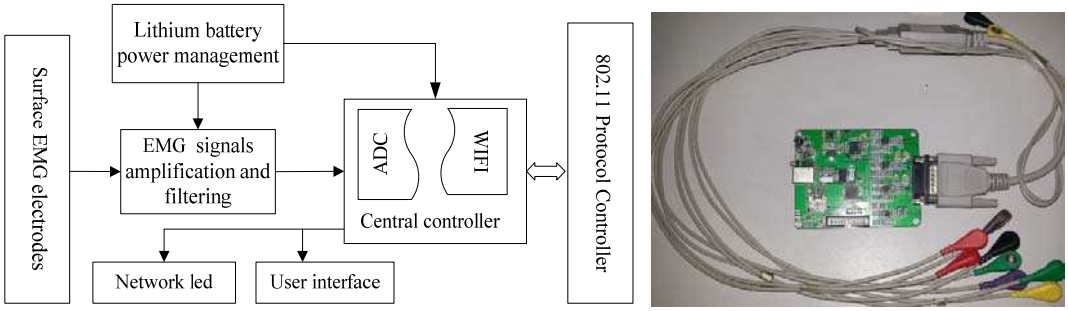

(a) systematic architecture *(b) hardware picture*

Figure 2 *The self-developed wireless EMG acquisition device.*

4. Motion Recognition and Muscle Activity Evaluation

4.1 EMG features extraction and motion recognition

EMG signals are often utilized to control the power-assist robot since they can directly reflect the user's movement intention and the muscle activity levels (Kiguchi *et al*., 2004). In recent years, a number of methods have been proposed to extract useful information from EMG signals (Ai *et al*., 2013). However, it is difficult to estimate the intended motions accurately from multichannel EMGs by using a fixed classifier. The existing methods tend to be complicated or require huge amount of signal samples, most of them for lower limb EMG signal are less than ideal and can not meet the real-time requirement. Since the coefficients of AR model contain sufficient features of EMG signals, they are selected as the features to model the motion patterns in this paper. The transfer function of AR model is defined as:

$$x(n)+\sum_{i=1}^{p} a_i x(n-i)=w(n) \tag{1}$$

where p is the order of the used AR model, a_i is the AR coefficients ($i = 1, 2, \cdots, p$), $x(n)$ is the EMG sample, and $w(n)$ is the residual value of white noise.

In this paper, four-channel EMG signals are collected and utilized for lower limb's motion recognition, so a four-order AR model is established in this context. That is:

$$\boldsymbol{a} = \{a_{11}, a_{12}, a_{13}, a_{14}, a_{21}, \cdots, a_{44}\} \tag{2}$$

The canonical equation of AR model is the Yule-Walker style, which builds the relationship between the AR coefficients a_i and the self-correlation matrix of $x(n)$.

$$\begin{bmatrix} R(0) & R(1) & R(2) & \cdots & R(p) \\ R(1) & R(0) & R(1) & \cdots & R(p-1) \\ R(2) & R(1) & R(0) & \cdots & R(p-2) \\ \vdots & \vdots & \vdots & \ddots & \vdots \\ R(p) & R(p-1) & R(p-2) & \cdots & R(0) \end{bmatrix} \begin{bmatrix} 1 \\ a_1 \\ a_2 \\ \vdots \\ a_p \end{bmatrix} = \begin{bmatrix} \sigma^2 \\ 0 \\ 0 \\ \vdots \\ 0 \end{bmatrix} \tag{3}$$

The equations above can be solved by the Levinson-Durbin based iterative algorithm as follows:

$$\sigma_k{}^2 = R(0) + \sum_{i=1}^{k} a_{k,i} R(i) \tag{4}$$

$$D_k = \sum_{i=0}^{k} a_{k,i} R(k+1-i), \qquad \gamma_{k+1} = \frac{D_k}{\sigma_k{}^2} \tag{5}$$

$$\sigma_{k+1}{}^2 = (1 - \gamma_{k+1}{}^2)\sigma_k{}^2 \tag{6}$$

$$a_{k+1,i} = a_{k,i} - \gamma_{k+1} a_{k,k+1-i}, \qquad a_{k+1,k+1} = -\gamma_{k+1} \tag{7}$$

With above equations (4)-(7), the AR coefficients a_i can be obtained, and they are used as the inputs to a classifier for motion recognition.

Support vector machine has gained wide acceptance in pattern recognition fields. It is shown that SVM is superior to other machine learning methods such as back propagation neural network (BPN), since SVM is able to gain better generalization ability for unseen data (Liu *et al*., 2007). In this study, a method based on the AR features of EMG in combination with a SVM classifier is proposed, which is quite effective for solving nonlinear classification problems and reducing computation time. Supposing the samples are $\{x_i, d_i\}$, where x_i is the sample to be classified, and d_i is the category of sample x_i. So the optimal hyper-plane $w^T x_i + b = 0$ should meet the formula and we need to find the minimum $\|w\|^2 / 2$, which can be rewritten as:

$$\begin{cases} y_i(w^T x_i + b) \geq 1, \quad i = 0, \ldots m \\ \min(J(w)) = \|w\|^2 / 2 \end{cases} \tag{8}$$

The objective function above is to find the optimal solution under inequality constraints, and this can be resolved by Lagrange functions:

$$L(w, b_0, \lambda) = \frac{1}{2} w^T w - \sum_{i=1}^{N} \lambda_i \left[y_i \left(w^T x_i + b_0 \right) - 1 \right] \tag{9}$$

where λ is the Lagrange multiplier, and finally we can obtain the classification function as:

$$f(x) = \operatorname{sgn}(\sum_{SV}^{m} y_i \lambda_i^* (x_i \cdot x) + b^*) \tag{10}$$

where x_i is the support vector, and λ_i^* is the Lagrange multiplier with respect to the support vector, and b^* is a constant. For nonlinear classification system, the slack variable $\xi \geq 0$ should be introduced, and the objective function becomes:

$$\begin{cases} J(w,\xi) = \dfrac{1}{2}(w \cdot w) + C\sum_{i=1}^{m} \xi_i \\ y_i[(w \cdot x_i) + b] - 1 + \xi_i \geq 0, \quad i = 1,...,m \end{cases} \tag{11}$$

where $C > 0$ is the penalty factor which is used to find the optimal hyper-plane under nonlinear conditions by transforming them to the samples suitable for linear classification.

Considering the nonlinear samples, the kernel function is utilized in nonlinear transformation to map the nonlinear variables to the high-dimensional linear space. Based on the features of EMG signals, a radial basis function (RBF) is selected as the kernel function here.

$$K(x,z) = \exp\left(-\frac{\|x-z\|^2}{\delta^2}\right) \tag{12}$$

4.2 Evaluation of muscle activity level

In order to provide the robot assistance based on patient's recovery conditions, the progressive rehabilitation should be considered by monitoring the patient's muscle condition and updating the robot controller in real time. As muscle activity levels are closely related to the coordination of multiple muscles, a number of researchers have used EMG signals to evaluate patient performance during the training or exercise sessions (Akdogan *et al*., 2012). However, the level of EMG readings may vary between different sessions. So in order to compensate this variability, the EMG signals have to be normalized. Moreover, there are different contributions of each muscle when conducting different motion patterns. Therefore, the weight coefficients of involved muscles of the limb have to be considered when evaluating the patient's muscle activity level.

The SVM classifier is utilized to predict movement intention in this paper, so the process can be divided into two stages: the training stage and the active testing stage. In the first stage, the subject is asked to keep a certain motion for a period of time, so that EMG signals can be sampled and used to train the SVM classifier. And in the second stage, the subject is asked to move the limb freely and the motion can be identified by the trained classifier. The EMG signals in the first stage can be regarded as the reference criterion to identify the movement intention, and thus it is also reasonable for that to be used for normalizing the muscle activity levels. The scheme of motion recognition and muscle activity evaluation based on EMG signals is illustrated in Figure 3. Specifically, in the training stage, for each motion pattern, the weight coefficients of four selected muscles are calculated based on the total RMS values of four-channel EMG signals.

$$w_i = \frac{\overline{RMS_i(n)}}{\sum \overline{RMS_i(n)}}, \qquad i = 1,2,3,4 \tag{13}$$

In the second stage, subjects are asked to perform an active movement task, and the EMG signals are used to identify the motion pattern and evaluate the muscular activity level for the immediate pattern. Because different motions activate different limb muscles, the patient's muscle activity level is calculated by integrating the normalized RMS values and the weight coefficients (Yin *et al*., 2012). In other words, when subjects intend to move, the limb's motion will be recognized by EMG signals, and as the weight coefficients of muscles contributing w_i have

been obtained in the training stage, so it is clear how much a muscle is involved in such a certain motion. And therefore it is more reasonable to evaluate the muscle activity level by integrating the normalized RMS values and the weight coefficients of activated muscles:

$$mal(n) = \sum_{i=1}^{n} w_i \cdot \frac{RMS_i(n)}{init(RMS_i)}, \quad i = 1,2,3,4 \tag{14}$$

where w_i is the weight coefficient of channel *i* for the current motion pattern, and $RMS_i(n)$ presents the RMS value of the *n*th sampled signals of channel *i*, $init(RMS_i)$ is the initial RMS value of channel *i*, which is equal to the average RMS of channel *i* ($\overline{RMS_i(n)}$) computed above. The average of RMS values of EMG signals and muscle activity levels are computed for each movement session, according to the total EMG values during this session and the period of time.

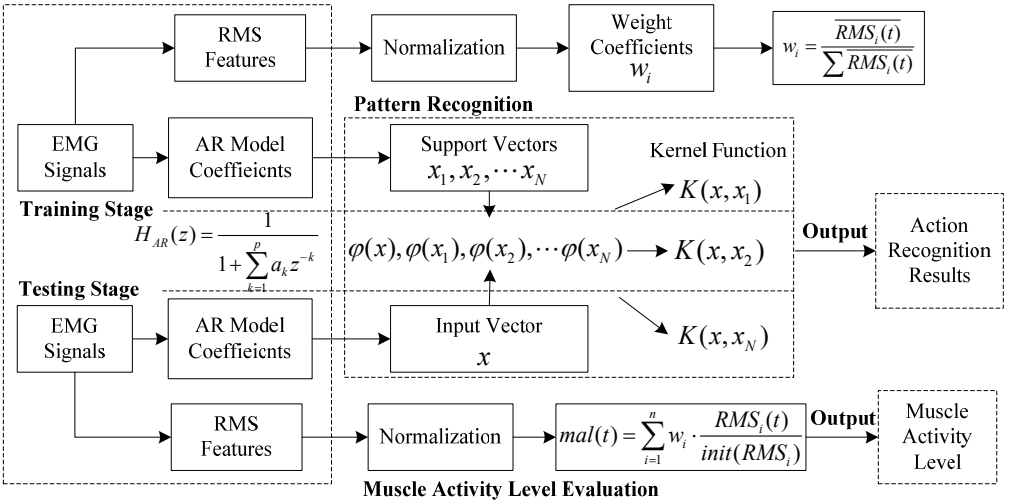

Figure 3 *Motion classification and muscle activity evaluation scheme based on EMG signals*.

5. Adaptive Impedance Control for Interactive Rehabilitation

The motion recognition system determines the rehabilitation trajectory and parameters based on real-time evaluation and motion decoding. In order to provide a compliment environment after the robot being triggered, flexible assistance should be provided by monitoring the interaction force between the user and the robot. Therefore, a position-based impedance model is established in this context. The robot can be controlled in admittance with the reference trajectory of the robot when the patient attempts to move. By measuring the interaction force applied by users, it is possible to compute the reference position/velocity required to render certain mass, stiffness, and damping parameters (Saglia *et al*., 2013). The control objective of this impedance controller is to modify the robot assistance movement in each direction of the task space with user's active interaction, so the dynamic relationship between the robot end-effector position and the interaction force needs to be established (Lopes and Almeida, 2008). In order to fulfill such task space requirements, a second-order, end-effector impedance model is chosen and expressed by Eq. (15).

$$\boldsymbol{M}_d(\ddot{\boldsymbol{x}} - \ddot{\boldsymbol{x}}_d) + \boldsymbol{B}_d(\dot{\boldsymbol{x}} - \dot{\boldsymbol{x}}_d) + \boldsymbol{K}_d(\boldsymbol{x} - \boldsymbol{x}_d) = \boldsymbol{F}_e \tag{15}$$

where $\boldsymbol{M}_d$, $\boldsymbol{B}_d$ and $\boldsymbol{K}_d$ are the diagonal matrices representing the desired inertia, damping, and stiffness parameters, $\boldsymbol{x}$ and $\boldsymbol{x}_d$ are the actual and the desired end-effector positions vectors in task space (Lopes and Almeida, 2008). $\boldsymbol{F}_e$ is the interaction force the user exerts upon the robot.

In this parallel robot-aided rehabilitation program, the end-effector's acceleration changes very slowly, so the impact of the acceleration change $\ddot{\boldsymbol{x}} - \ddot{\boldsymbol{x}}_d$ may be ignored (Xu *et al.*, 2011). Considering the actions of desired stiffness and damping, Eq. (15) can be simplified as:

$$\boldsymbol{B}_d(\dot{\boldsymbol{x}} - \dot{\boldsymbol{x}}_d) + \boldsymbol{K}_d(\boldsymbol{x} - \boldsymbol{x}_d) = \boldsymbol{F}_e \tag{16}$$

The traditional impedance controller imposes fixed parameters on the patient and can not adapt the impedance to different users. While it is widely accepted that the rehabilitation should consider the patient's recovery condition and update the impedance parameters in real time. Since impedance parameters of the human limb will be changed for different muscle activity levels, therefore, the robot impedance should be changed depending on the activity levels (Kiguchi and Hayashi, 2012). In the proposed controller, impedance parameters of the robot are adaptable in accordance with the active ratio of lower-limb muscles to realize the natural and adaptive assist compliance. As mentioned above, in order to guarantee the assistive trajectory to be physiological, this impedance controller works with a constant reference trajectory and only adapts the robot velocities. The desired damping is the most important factor when an impedance model following force and velocity control is applied, and it is also one of the impedance parameters acts as a velocity feedback gain (Nagata *et al.*, 2009). On the other hand, in the force-controlled work space, if only a simple force feedback is applied, the response can be under-damped for an environment with high stiffness under rigid conditions (Patel and Shadpey, 2005). So we introduce a method for tuning the desired damping parameters here, and similar strategies applied in robot compliance control can also be found in related works from Cho and Park (2005), Hu *et al.* (2012), or Saglia *et al.* (2013). Note that the inertia has been set to zero, and in the case of pure damping simulation, a proper stiffness is selected necessary to ensure the system stability. This guarantees that the user interacts with the external environment with a velocity that can be properly adjusted by the impact forces. Therefore, the viscous damping of impedance controller is the parameter to be adjusted, while the stiffness is selected properly, depending on the muscle activity levels of lower-limb. The trajectories will not be modified and the damping parameter $\boldsymbol{B}_d$ is adjusted as follows:

$$\boldsymbol{B}_d = \boldsymbol{B}_0 + \lambda \boldsymbol{C}_{EMG}, \qquad \lambda = \mathrm{sat}(mal(n)) \tag{17}$$

where $\boldsymbol{B}_0$ is initial viscous damping matrix for the initial position, $\boldsymbol{C}_{EMG}$ is the proportional coefficient matrix of EMG effects, and $mal(n)$ is the muscle active level evaluated by Eq. (14). $\mathrm{sat}(\cdot)$ is a saturation function. Thus, the amount of damping parameter $\boldsymbol{B}_d$ is increased when the activity level of related lower-limb muscles simultaneously increased. And velocities of the robot are set to be proportional to active interaction force based on damping parameter.

The controller architecture for damping-active training is shown in Figure 4. The outer loop is an impedance control loop with damping parameter, and the inner loop is a position/velocity controller. The damping coefficient is changed for different training resistances according to the muscle activity level, which is identified by EMG signals considering the weight coefficients of involved muscles in different motion patterns. Furthermore, the adaptive controller is proposed to adjust the impedance parameters and influence the robot speed in accordance with the patient's interactive efforts. Specifically, a fuzzy PID adaptive controller was implemented in joint space as a basic position/velocity controller of the 6-DOF parallel robot, and the detailed implementation of such controller can be found in our previous work (Zhou *et al*., 2013).

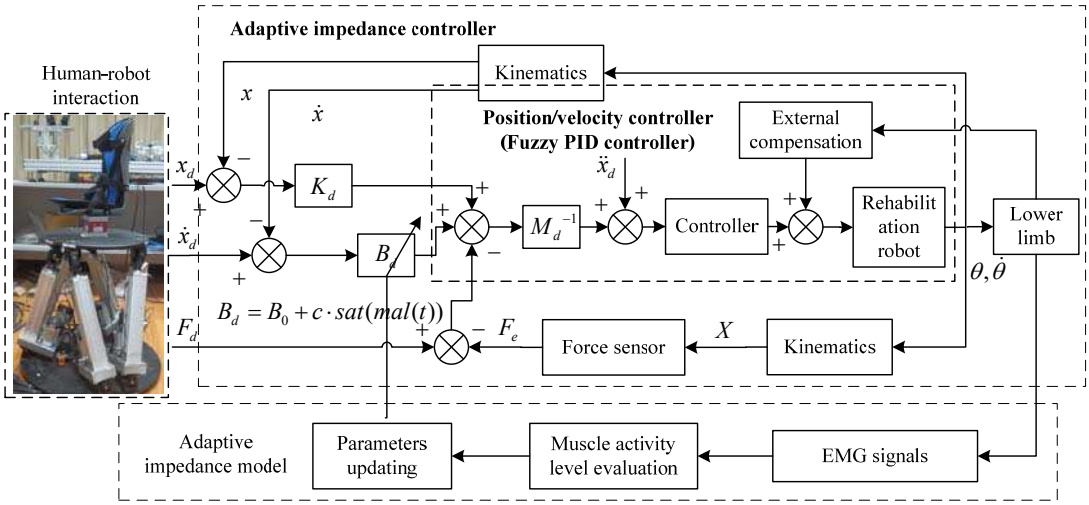

Figure 4 *Adaptive impedance control based on muscle activity level evaluation.*

6. Experiments and Results

6.1 Experimental Setup

In order to evaluate the ability of the integrated parallel rehabilitation robot to provide interactive rehabilitation for lower limbs, the previously described robot and controller were implemented in a preliminary experiment. Information including EMG signals, robot position, velocity and the interaction force are collected and analyzed. The surface EMG signals are acquired by the self-developed wireless EMG acquisition device based on Wi-Fi, with a 60db amplifier, a 20~500Hz band pass filter, a 50Hz notch filter, and an A/D convertor. A Futek force sensor (MTA400 tri-axial load cell, Advanced Sensor Technology, INC. USA) is mounted between the moving platform and the footplate to sense the interaction force acting between human and robot. The force signals are amplified before being sent to the PC by the Futek amplifier modules and a low pass filter is used to tune the system in order to minimize the effect of noises.

The experiments were carried out with nine subjects aged range from 20 to 42, including both male and female subjects. Six motions of lower limb that are frequently used, namely, dorsiflexion, plantarflexion, inversion, aversion, adduction, and abduction (Jamwal *et al*., 2014) were adopted. Four-channel EMG signals from the subject's gastrocnemius medialis (GM), tibialis anterior (TA), flexor digitorum longus (FDL) and soleus (SL) muscles were captured. The location of electrodes is shown in Figure 5(b). The surface EMG signals of these muscles were acquired in real time, and the force sensor was located to understand the human robot interaction. The subjects sat on a chair with his/her right foot constrained to the robotic device, as illustrated in Figure 5(c). Considering the safety issue, this preliminary test was performed with healthy subjects. This experiment was designed to evaluate if the proposed control scheme could trigger the robot assistance and modify the robot movement based on subject's EMG signals and active efforts. Since the participation of healthy subjects and patients are both indicated by the data from force sensors and EMG, it is reasonable to verify the effectiveness of the proposed method by experiments on healthy subjects, and this is also accepted by many works such as Hussain *et al.* (2013) and Kiguchi *et al.* (2012).

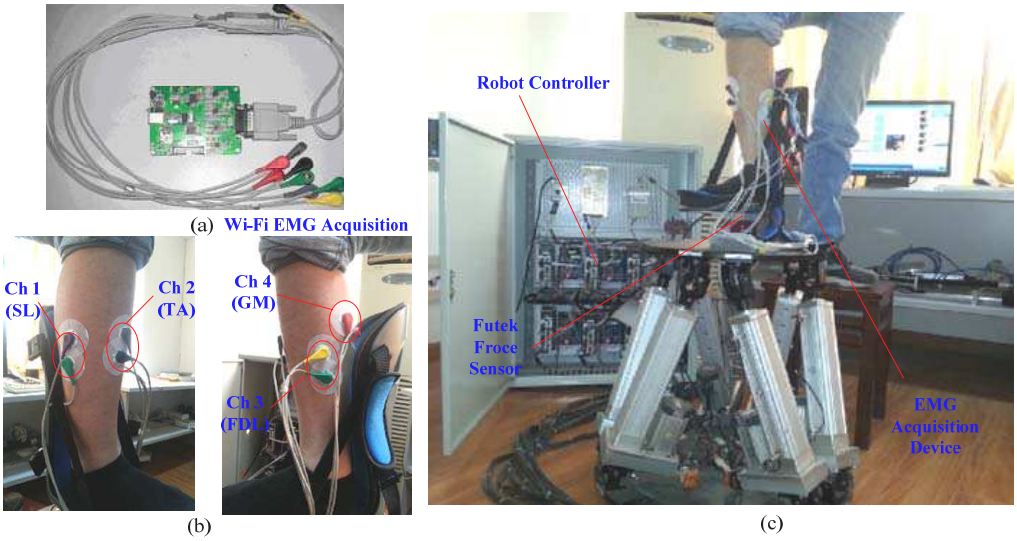

Figure 5 *(a) Wi-Fi EMG acquisition device (b) location of EMG electrodes (c) experimental setup*

The experiment process of the proposed method contains four main steps (see Figure 6):

(1) EMG signals acquisition and processing, with filtering and amplification. The four-channel surface EMG signals from lower limb were acquired by using the self-developed wireless EMG acquisition device, and the raw signals were transmitted to the PC for further processing via Wi-Fi protocol. Specifically, we used Ag/AgCl bipolar electrodes with a conductive diameter of 16 mm, and the inter-electrode distance was set to 20 mm. The EMG signals were digitized by an A/D converter (sampling frequency, 1 kHz; quantization, 12 bit) after being amplified (60 dB) and filtered through a band-pass filter (20~500Hz) and a notch filter (50 Hz).

(2) Motion prediction and muscle activity level evaluation by using EMG signals. The experiment consists of two parts. In the first part, the subject was asked to perform the six motions one by one and maintain it for fifteen seconds so that the EMG dataset can be acquired to train the SVM. The SVM classifier was implemented by C++ language. The SVM training time was less than 100 ms and can be ignored compared to the subject's movement duration. In the second part, the trained SVM was used to on-line recognize the movement intention and control the robot. In this part, the subject was asked to perform continuous movements. The robot assistance will be triggered once the subject's movement intention is identified, and the muscle activity level was calculated simultaneously based on the normalized EMG signals and weight coefficients.

(3) Updating of impedance parameters and velocity commands. An adaptive impedance control law was proposed to relate the muscle activity level to the damping parameter, so that the robot assistance speed can be adjusted in accordance with the human interaction force and the recovery conditions. The concept behind this adaptive law is to set the robotic damping low if low muscle activity level is detected from the subject. This low impedance will increase the robot speed under the same interaction force to make the subject change the training speed more easily. Similarly, the damping of the robot is adapted to be high if the subject shows a higher muscle activity level. This high impedance allows the subject to participate more voluntary efforts to deviate the robot from the reference speed during exercise.

(4) Following the predefined trajectory and generating the adaptive robot velocity based on inverse kinematics and fuzzy PID controller, which was implemented in joint space as a basic position/velocity controller of the 6-DOF parallel robot to guide the subject's limb on reference

trajectories. We refer the reader to (Zhou *et al*., 2013) for the detailed implementation of such controller for parallel robotic manipulator. In this experiment, the position and velocity tracking results of the robot have showed satisfactory control performance for rehabilitation purpose. The average joint position tracking errors and velocity tracking errors were controlled to less than 1mm and 0.1 mm/s, respectively, and the plots can be found in (Zhou *et al*., 2013).

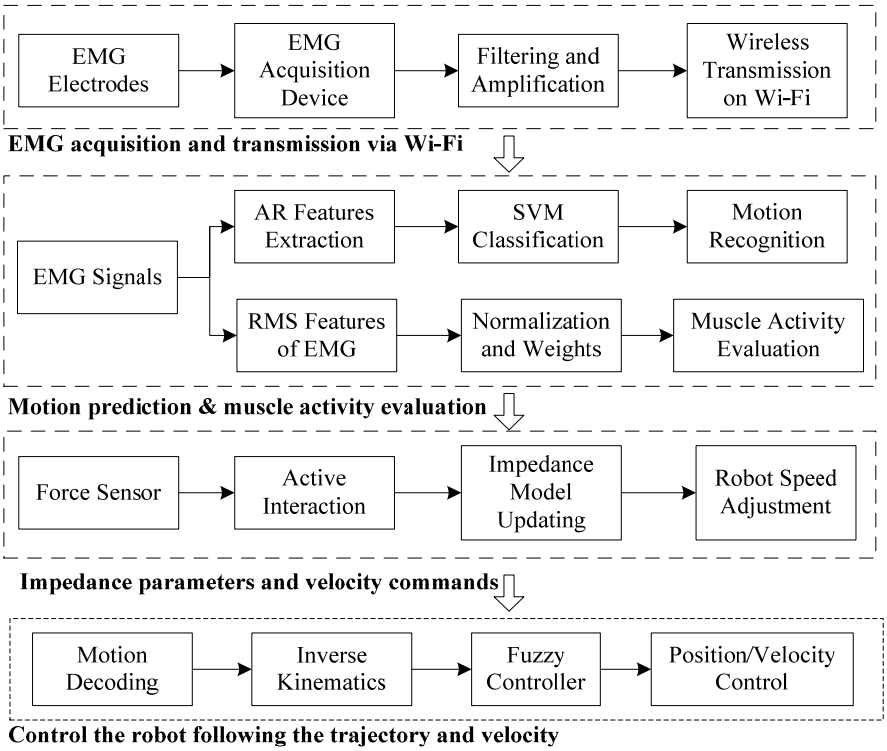

Figure 6 *Four main steps of rehabilitation robot control process in this study*

Experiments were carried out to demonstrate the comparison of conventional EMG-triggered control method and the proposed method. In the first trial, the subjects were asked not to exert any force and remain passive after the robot being triggered by EMG signals. In the second trial, experiments on the proposed method were executed, where the impedance parameters are adjustable to allow the subjects to change the robot compliance by themselves. The subjects were instructed to perform voluntary movements and contribute their muscular forces in the training. The primary goal of the first trial was to determine if the EMG-based controller can identify the user's movement intention and trigger the robot assistance, and the primary goal of the second trial was to determine whether the proposed active interaction controller can improve the user's voluntary participation and increase the muscle activity levels. Although the motions can be classified continuously in any order, the subject in this test was asked to perform the motions from dorsiflexion to abduction one by one. Each motion took about 10 seconds. Each subject was asked to undergo six movement sessions and each session had 6 continuous motions (dorsiflexion, etc.). Meanwhile, all experiments were conducted with the first trial and the second trial for comparison. In addition, the subject was asked to have a 3 minutes rest between two movement sessions.

6.2 Results and Discussion

Firstly, we examined the EMG motion recognition ability. After training the SVM in the first part of the trial, the EMG signals of four channels were acquired and transmitted to the processing

part, where we identified the user's movement intention based on AR features extraction and SVM classification. The experiment program was written by C++ language and run on a PC with dual 2.8 GHz CPU. The motion recognition results can be output 20 ms in advance before the subject is starting to move his/her leg. In other words, the subject's movement intention can be identified 20ms earlier to the people's actual movement. Once the movement intention was determined, the robot assistance will be triggered immediately. The communication between the EMG recognition part and the robot part was realized by TCP protocol. So, there was a time delay of about 50 ms before the robot was reacting. Actually, there will be around 30ms delay when people attempt to drive the robot by their own efforts, this, however, may not be noticed by the subjects in actual experiment. In fact, the subjects found they can drive the robot immediately when they intended to move and they can adapt the robot control during the whole movement.

In this experiment, the subject was suggested to perform the six continuous motions from dorsiflexion to abduction in order to facilitate the comparison between different trials, which also made it easier to verify the classifier's ability to identify the movement types continuously. Figure 7 shows an example of the partial results for Subject2 (S2), Subject5 (S5), and Subject8 (S8). The captured four-channel EMG signals and classification results are demonstrated. In order to further evaluate the effectiveness of the classifier, more experiments were performed with a group of nine healthy subjects. In this part, each subject was instructed to undergo total 50 movement recognition trials. The recognition details of all subjects are illustrated in Table I. A statistical overview of motion recognition results, described by means of the average accuracy and standard deviation (SD), was reported for each subject in Table I. In the case of S1 and S6, the average recognition accuracy is higher than others because these two subjects had been participated in our experiment for a long time and they were very familiar with experimental protocol. In contrast, the results of S2, S7 and S9 are relatively unsatisfactory, partially due to the muscle activity variations with gender and age and partially because they didn't perform the motions accurately. Regarding to other four subjects (S3, S4, S5, S8), although their EMG signals of lower limb are very different with each other, the motion recognition results of them are all satisfied, which prove the reliability and adaptability of the proposed prediction methods. The results of almost all subjects suggest that the EMG feed forward items and SVM method makes it possible to precisely predict human motion intention in advance and the satisfactory motion recognition accuracy (the subjects' average rate of success is 94.71±2.83%) can be obtained, especially for several motions such as dorsiflexion, plantarflexion, and abduction, in which the success rate can reach above 95%.

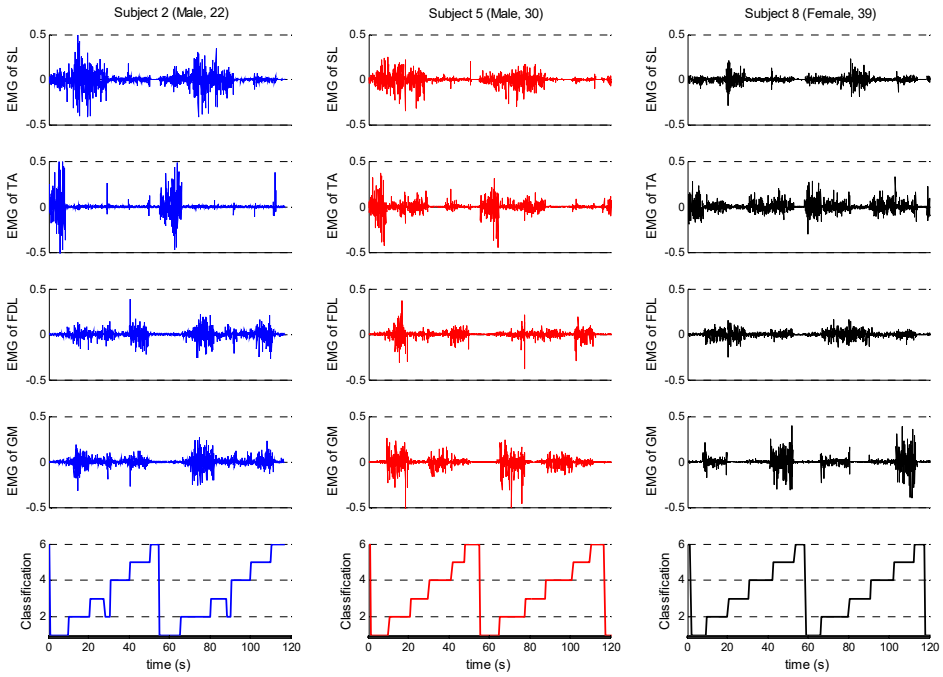

Figure 7 *The EMG signals and motion recognition results of S2, S5, and S8 in active control mode. Each figure show the EMG signals (mV) of SL, TA, FDL and GM muscles during the movement and the classification results, in which the numbers from 1 to 6 present the six motions including dorsiflexion, plantarflexion, inversion, aversion, adduction, and abduction, respectively.*

Table I *Statistical analysis of motion recognition results with nine healthy subjects*

Subjects	Gender	Age	Recognition results of six motions (correct times / total times)						Average Accuracy
			dorsiflexion	plantarflexion	inversion	aversion	adduction	abduction	
S1	Male	20	48/50	48/50	49/50	47/50	49/50	49/50	96.67±1.63%
S2	Male	22	47/50	46/50	44/50	47/50	48/50	49/50	93.67±3.44%
S3	Female	25	49/50	47/50	48/50	48/50	47/50	48/50	95.67±1.51%
S4	Female	27	47/50	48/50	49/50	49/50	46/50	47/50	95.33±2.42%
S5	Male	30	47/50	49/50	46/50	48/50	45/50	48/50	94.33±2.94%
S6	Male	33	50/50	50/50	48/50	46/50	48/50	49/50	97.00±3.03%
S7	Female	37	48/50	47/50	44/50	45/50	46/50	44/50	91.33±3.27%
S8	Female	39	46/50	48/50	48/50	47/50	49/50	47/50	95.00±2.10%
S9	Male	42	47/50	45/50	46/50	49/50	44/50	49/50	93.33±4.13%
Average Accuracy			95.33%	95.11%	93.78%	94.67%	93.78%	95.56%	94.71±2.83%

Secondly, the robot impedance tuning and robot control process in proposed active mode were presented and analyzed. The objective is to demonstrate how the robot compliance can be tuned according to people's muscle activity level and how the robot movement velocity can be influenced by the subject's active interaction force. In this part, we just try to verify the robot impedance tuning and active control process by using the proposed method, while the comparison between the two modes will be discussed in next section. Although the muscle activity levels and interaction forces vary a lot to different subjects, the parameter tuning and robot control process are similar for all subjects. Without loss of generality and for simplicity's sake, experimental

results of three subjects are selected from nine. The experimental results of S2, S5 and S8 during the exercise with assist of robot controlled by the proposed mode are illustrated in Figure 8, where the muscle activity level, the shaped impedance parameter, the active interaction force, as well as the robot velocity tracking results are demonstrated. From the results, one can see that the robot impedance (damping here) can be adjusted by the user's muscle activity levels, and the robot movement velocity was determined by both the human-robot interaction force and the damping parameter. Specifically, the robot can be compliant (a lower damping) when the muscle activity level is low, while the robot's damping will increase when the subject shows a higher muscle activity level. Meanwhile, the robot movement speed was greatly influenced by subject's active interaction force (a larger interaction force yielded a higher robot velocity), which encourages the users to contribute their own efforts during the exercise. In addition, the desired and the actual velocity tracking results are also shown in Figure 8, where the solid line is the desired velocity and the dotted green line is the actual one. It can be seen that the tracking accuracy of the controller is satisfied for such a parallel robot, and more details can be found in (Zhou *et al.*, 2013).

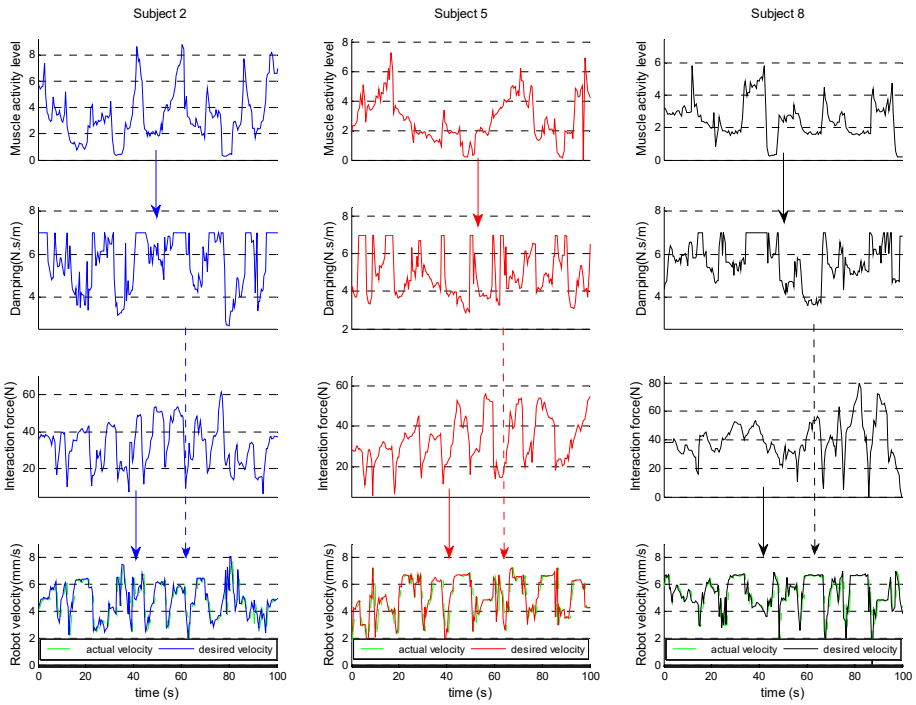

Figure 8 *The impedance tuning and robot control process considering the interaction force and muscle activity levels of S2, S5, and S8 in active mode. For each subject, the impedance parameter (damping here) was shaped by the user's muscle activity level (as the arrow indicates). The robot velocity was determined by the human-robot interaction force and the damping parameter tuned above (as the two arrows indicate). In the plots of robot velocity, the solid line is the desired velocity and the dotted green line is the actual velocity.*

Thirdly, we analyzed the experimental results to determine whether the proposed active interaction controller could improve the user's voluntary participation, i.e. whether the proposed approach increases muscle activity levels. To this ends, we compared the differences in muscle activity levels between the proposed and traditional methods. The experimental results of subjects

(1-9) are shown in Figure 9. This figure shows that the both types of values of the active mode were higher than the traditional mode. Additionally, Table II shows the average of 6 sessions in the RMS values and muscle activity levels for each training mode and for each subject. Both Figure 9 and Table II show a distinct increase of both types of muscle activity values (muscle activity level and RMS value) for the active mode compared to the traditional mode. Taking S1 for example, the overall average muscle activity level and RMS value in EMG-triggered mode are 3.982±0.509, 1.445±0.245, respectively, while the average values in active mode are 5.857±0.594, 3.076± 0.549, respectively, in which the rates of increase are 47.08% and 112.8% when compared to the previous one. These results show that the proposed active control methods can be realized with a higher level of the people's active participation rate. The similar results were also obtained with other subjects. Although different subjects yielded different rates of increase in muscle activity levels and RMS values, the improvements of their active participation and muscle activities are all obvious, indicating that the proposed method is applicable to any users. The experimental results show that the active interaction controller can increase the amount of the muscle activity levels for each movement session compared to the traditional mode. This would allow patients to contribute more efforts during the exercise and may increase the training effects.

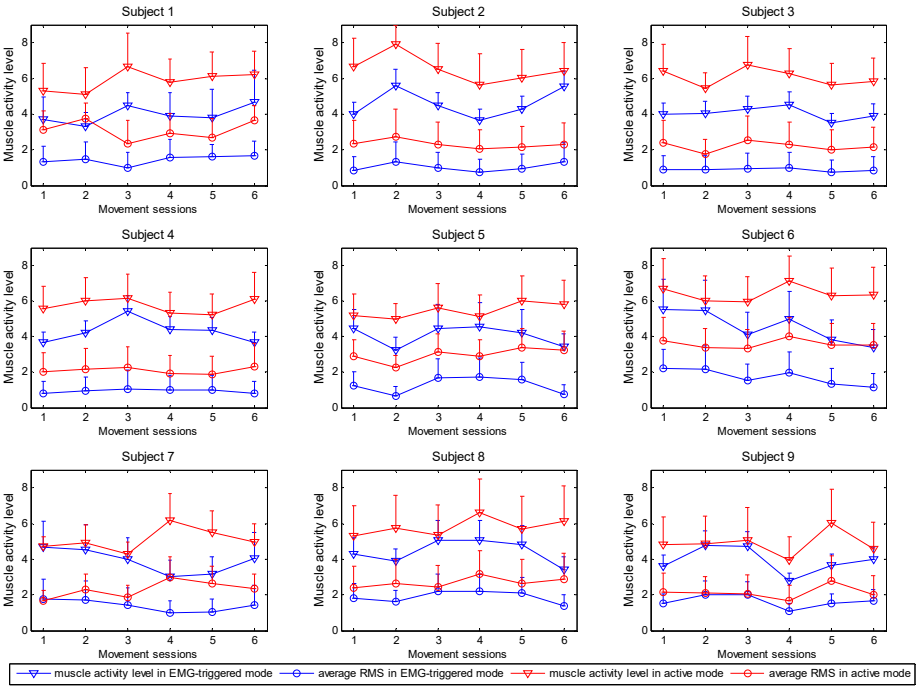

Figure 9 *The muscle activity level for each training mode (active/traditional), each type of muscle activity value (RMS/muscle activity level), and each subject within one of six movement sessions. Every subject was instructed to undergo six movement sessions (each session had 6 motions) for both modes. For each session, the average muscle activity levels and the RMS values as well as the standard deviations are presented. The red lines are the two types of muscle activity value in active mode, while the blue lines are the muscle activity values in EMG-triggered mode.*

Table II *shows the average of 6 movement sessions for each training mode, each type of muscle activity value, and each subject. Additionally the rate of increase of the active mode compared to the traditional mode is shown for each muscle activity value (RMS/muscle activity level).*

	Traditional EMG-triggered mode				The proposed active mode					
	Muscle activity level		RMS value		Muscle activity level			RMS value		
Subjects	Mean	SD	Mean	SD	Mean	SD	Increase	Mean	SD	Increase
S1	3.982	0.509	1.445	0.245	5.857	0.594	47.08%	3.076	0.549	112.8%
S2	4.593	0.799	1.041	0.246	6.528	0.768	42.12%	2.314	0.236	122.3%
S3	4.041	0.348	0.896	0.087	6.057	0.512	49.88%	2.205	0.281	146.1%
S4	4.284	0.644	1.124	0.100	5.724	0.408	33.61%	2.088	0.185	85.76%
S5	4.054	0.571	1.266	0.272	5.452	0.413	34.48%	2.578	0.386	103.6%
S6	4.551	0.894	1.726	0.347	6.397	0.447	40.56%	3.587	0.255	107.8%
S7	3.907	0.674	1.396	0.335	5.089	0.665	30.25%	2.298	0.366	64.61%
S8	4.417	0.658	1.887	0.329	5.802	0.500	31.35%	2.684	0.286	42.24%
S9	3.913	0.751	1.635	0.346	4.874	0.470	24.56%	2.129	0.356	30.21%

During the EMG-triggered assistance trial, the subject kept passive after activating the robot by EMG action recognition, so the muscle activity is at lower level during this movement except for when people trying to trigger the robot. Differently, in the active interaction assistance trial, the subject had to provide a certain effort to keep the robot move in agreement with his/her intention, so the selected muscles will be activated for a long period of time. In the proposed method, the robot compliance can be adjusted according to his/her muscle activity level while the traditional method does not take the subject's status into account. It is clear that there was a distinct increase in the muscle activity levels for all subjects with the active interaction mode, compared to the EMG-triggered mode. The increase in RMS values indicated that the active mode had a positive effect in encouraging muscle activation. On the other hand, the muscle activity level evaluation calculated here takes into account the muscles' weight coefficients in a certain motion. The weight coefficients were determined in the SVM training stage and were calculated by using Eq. (14). The obtained muscles' weight coefficients of several subjects are illustrated in Table III. In order to simplify the table, three subjects are selected from nine. The objective of this table is to present the differences of muscles' weight coefficients in different motion patterns. Other subjects' data were not listed for simplicity's sake, but all data were obtained by using Eq. (13). Consequently, the muscle activity level here not only depends on the normalized EMG signals, but also considers the weight coefficients of each muscle in a certain motion pattern, so a more scientific model can be achieved and this can be adaptable to different people.

Table III *Muscles' weight coefficients of the subjects in different motion patterns.*

Motion patterns	Subject 2				Subject 5				Subject 8			
	SL	TA	FDL	GM	SL	TA	FDL	GM	SL	TA	FDL	GM
dorsiflexion	0.176	0.701	0.082	0.041	0.252	0.638	0.043	0.067	0.159	0.751	0.057	0.033
plantarflexion	0.173	0.083	0.441	0.303	0.271	0.133	0.107	0.489	0.123	0.153	0.350	0.374
inversion	0.526	0.192	0.253	0.029	0.493	0.326	0.132	0.049	0.516	0.101	0.352	0.031
aversion	0.178	0.640	0.106	0.076	0.369	0.104	0.106	0.421	0.115	0.615	0.161	0.109
adduction	0.106	0.067	0.316	0.511	0.095	0.193	0.488	0.224	0.065	0.063	0.147	0.725
abduction	0.293	0.234	0.255	0.218	0.172	0.122	0.408	0.298	0.236	0.268	0.212	0.284

EMG-triggered robot assistance and real-time adjustment of impedance during the training have been demonstrated previously in (Emken *et al*., 2008) and (Xu *et al*., 2011). However, the method proposed here differs in three main ways. Firstly, it provides a seamless interaction control scheme for robot-assisted rehabilitation after activating the robot by motion recognition. Both

subject's movement intention and voluntary participation are considered, not only triggering the robot when the user intends to move, but also changing the motion pattern in accordance with the user's participation efforts during the movement. In contrast, the existing EMG-triggered approach is to provide assistance when the subject starts the movement but remain passive after the robot is triggered. Secondly, the impedance controller developed here is different in that it responds to velocity changes rather than variations in trajectory, and thus only allows freedoms in the training speed and keeps the movement along a physiological trajectory. Moreover, the algorithm proposed here adapts the robot impedance as a function of the user's muscle activity level. On the contrary, the existing algorithms always limited the robot speeds but changed the path severely, which may guide the impaired limb move along an un-physiological pattern. Thirdly, as muscles have different contributions in conducting different motion patterns, the muscle activity evaluation here takes into account the muscles' weight coefficients in a certain motion pattern (as described in Table III) and thus a more scientific model can be achieved. By using the proposed method, the robot can be compliant if the patient has severe impairment with low muscle activity so that the patient can influence the robot movement more easily. On the other hand, the robot behavior can be made stiff if the patient shows high muscle activity level so that the patient can contribute more efforts to the training process. Consequently, the proposed active interaction control strategy can adapt the robot compliance by adjusting an impedance model from movement to movement based on the patient's muscle activity levels and the recovery conditions.

7. Conclusion

In summary, this paper presents a seamless active interaction control method between the EMG-triggered assistance and the adaptive impedance control scheme for parallel robot-assisted lower limb motor exercise and training. Both people's movement intention and voluntary efforts are considered, not only triggering the robot assistance when user attempts to move, but also changing the motion pattern in accordance with people's efforts during the movement. Firstly, a wireless EMG acquisition device based on Wi-Fi protocol was developed and a motion recognition method integrating AR coefficients and SVM classifier is proposed to identify the user's movement intention. Secondly, an impedance control method in accordance with the people's interactive efforts is implemented to make the robot compliant. Thirdly, the proposed method adapts the robot impedance as a function of people's muscle activity level, which considers the weight coefficients of each muscle in a certain motion pattern. Experimental results with several healthy subjects demonstrated that the robot was able to move coordinately with the user's intention while the impedance can be updated with the muscle conditions. It is clear that there was a distinct increase in the muscle activity levels for all subjects with the active interaction control mode, compared to the EMG-trigged mode. Such strategies will potentially increase the patient's motivation because the muscle activity level can change the robot compliance while the active efforts can be reflected in the training speed and thus can cause a consistent feeling of success.

Acknowledgments

This work was supported by the National Natural Science Foundation of China ("Research on sEMG-based Muscular Force Prediction Model and Interactive and Adaptive Impedance Control Approaches for Lower Limb Rehabilitation Robot") and the Fundamental Research Funds for the Central Universities (Grant Nos. 2013-YB-002 and 2013-IV-129).

References

Ai, Q. S., Liu, Q., Yuan, T. T. and Lu, Y. (2013), "Gestures recognition based on wavelet and LLE", *Australasian Physical & Engineering Sciences in Medicine*, Vol. 36 No.2, pp. 167-176.

Ai, Q. S., Chen, L., Liu, Q., and Zou, L. (2014), "Rehabilitation assessment for lower limb disability based on multi-disciplinary approaches", *Australasian Phys. & Eng. Sciences in Medicine*, Vol. 37 No.2, pp. 355-365.

Akdogan, E., Shima, K., Kataoka, H., Hasegawa, M. and et al. (2012), "The Cybernetic Rehabilitation Aid: Preliminary Results for Wrist and Elbow Motions in Healthy Subjects", *IEEE Transactions on Neural Systems and Rehabilitation Engineering*, Vol. 20 No.5, pp. 697-707.

Benitez, L. M. V., Tabie, M., Will, N., Schmidt, S. and et al. (2013), "Exoskeleton Technology in Rehabilitation: Towards an EMG-Based Orthosis System for Upper Limb Neuromotor Rehabilitation", *Journal of Robotics*, Vol. 2013 Article ID 610589, 13 pages, doi:10.1155/2013/610589.

Cho, H. C. and Park, J. H. (2005), "Impedance control with variable damping for bilateral teleoperation under time delay", *JSME International Journal Series C Mechanical Systems, Machine Elements and Manufacturing*, Vol. 48, No. 4, Special Issue on Bioengineering, pp. 695-703.

DiCicco, M., Lucas, L. and Matsuoka, Y. (2004), "Comparison of control strategies for an EMG controlled orthotic exoskeleton for the hand", in *Proceedings of the IEEE International Conference on Robotics and Automation* (ICRA '04), pp. 1622–1627.

Duchaine, V. and Gosselin, C. M. (2007), "General Model of Human-Robot Cooperation Using a Novel Velocity Based Variable Impedance Control", in *EuroHaptics Conference and Symposium on Haptic Interfaces for Virtual Environment and Teleoperator Systems. World Haptics* 2007, pp. 446-451.

Emken, J. L., Harkema, S. J., Beres-Jones, J. A., Ferreira, C. K. and Reinkensmeyer, D. J. (2008), "Feasibility of manual teach-and-replay and continuous impedance shaping for robotic locomotor training following spinal cord injury", *IEEE Transactions on Biomedical Engeering*, Vol. 55 No.1 , pp. 322-334.

Fan, Y. and Yin, Y. (2013), "Active and Progressive Exoskeleton Rehabilitation Using Multi-Source Information Fusion from sEMG and Force & Position-EPP", *IEEE Transactions on Biomedical Engineering*, Vol. 60 No. 12, pp. 3314-3321.

Fukuda, O., Tsuji, T., Kaneko, M. and Otsuka., A. (2003), "A Human-Assisting Manipulator Teleoperated by EMG Signals and Arm Motions". *IEEE Transactions on Robotics and Automation*, Vol. 19, No. 2, pp. 210-222.

Hu, J., Hou, Z., Zhang, F. Chen, Y. and et al. (2012), "Training Strategies for a Lower Limb Rehabilitation Robot Based on Impedance Control". in *34th Annual International Conference of the IEEE EMBS*, pp. 6032-6035.

Hussain, S., Xie, S. Q. and Liu, G. (2011), "Robot assisted treadmill training: Mechanisms and training strategies", *Medical Engineering & Physics*, Vol. 33 No.5, pp. 527-533.

Hussain, S., Xie, S. Q. and Jamwal, P. K. (2013), "Robust Nonlinear Control of an Intrinsically Compliant Robotic Gait Training Orthosis", *IEEE Transactions on Systems Man Cybernetics-Systems*, Vol. 43 No.3, pp. 655-665.

Jamwal, P. K., Xie, S. Q., Hussain, S. and Parsons, J. G. (2014), "An Adaptive Wearable Parallel Robot for the Treatment of Ankle Injuries", *IEEE/ASME Transactions on Mechatronics*, Vol. 19 No.1, pp. 64-75.

Ji, X. F. and Liu, H. H. (2010), "Advances in View-Invariant Human Motion Analysis: A Review", *IEEE Transactions on Systems Man and Cybernetics Part C-Applications and Reviews*, Vol. 40 No.1, pp. 13-24.

Ju, Z., Ouyang, G., Wilamowska-K., M. and Liu, H. (2013), "Surface EMG based Hand Manipulation Identification via Nonlinear Feature Extraction and Classification", *IEEE Sensor Journal*, Vol. 13 No. 9, pp. 3302-3311.

Kiguchi, K., Tanaka, T. and Fukuda, T. (2004), "Neuro-fuzzy control of a robotic exoskeleton with EMG signals", *IEEE Transactions on Fuzzy Systems*, Vol. 12 No.4, pp. 481-490.

Kiguchi, K. and Hayashi, Y. (2012), "An EMG-Based Control for an Upper-Limb Power-Assist Exoskeleton Robot", *IEEE Transactions on Systems Man and Cybernetics B-Cybernetics*, Vol. 42 No. 4, pp. 1064-1071.

Krebs, H. I., Palazzolo, J. J., Dipietro, L., Volpe, B. T., et al. (2003), "Rehabilitation robotics: Performance-based progressive robot-assisted therapy", *Autonomous Robots*, Vol. 15 No.1, pp. 7-20.

Lenzi, T., De Rossi, S. M., Vitiello, N. and Carrozza, M. C. (2012), "Intention-Based EMG Control for Powered Exoskeletons". *IEEE Transactions on Biomedical Engineering*, Vol. 59, No. 8, pp. 2180-2190.

Liu, Y.-H., Huang, H.-P. and Weng, C.-H. (2007), "Recognition of electromyographic signals using cascaded kernel learning machine", *IEEE-ASME Transactions on Mechatronics*, Vol. 12 No.3, pp. 253-264.

Liu, H. H. (2011), "Exploring human hand capabilities into embedded multi- fingered object manipulation", *IEEE Transactions on Industrial Informatics*, Vol. 7 No.3, pp. 389-398.

Lopes, A. and Almeida, F. (2008), "A force-impedance controlled industrial robot using an active robotic auxiliary device", *Robotics and Computer-Integrated Manufacturing*, Vol. 24, No.13, pp. 299-309.

Marchal-Crespo, L. and Reinkensmeyer, D. J. (2009), "Review of control strategies for robotic movement training after neurologic injury", *Journal of Neuroengineering and Rehabilitation*, Vol. 6 No. 20, pp.1-1.

Mobasser, F., Elklund, J. M. and Hashtrudi-Zaad, K. (2007), "Estimation of elbow-induced wrist force with EMG signals using fast orthogonal search", *IEEE Transactions on Biomedical Engineering*, Vol. 54, pp. 683-693.

Nagata, F., Hase, T., Haga, Z., Omoto, M. and et al. (2009), "A desktop NC machine tool with a position/force controller using a fine-velocity pulse converter", *Mechatronics,* vol. 19, No. 5, pp. 671 – 679.

Ouyang, G., Zhu, X., Ju, Z. and Liu, H. (2014), "Dynamical Characteristics of Surface EMG Signals of Hand Grasps via Recurrence Plot", *IEEE Journal of Biomedical and Health Informatics*, Vol. 18 No. 1, pp. 257-266.

Patel, R. V. and Shadpey, F. (2005), "Contact Force and Compliant Motion Control", in *Control of Redundant Robot Manipulators*, LNCIS 316, Springer-Verlag Berlin Heidelberg, pp. 79-117.

Riener, R., Lunenburger, L., Jezernik, S., Anderschitz, M., and et al. (2005), "Patient-cooperative strategies for robot-aided treadmill training: First experimental results", *IEEE Transactions on Neural Systems and Rehabilitation Engineering*, Vol. 13 No.3, pp. 380-394.

Riener, R., Luenenberger, L., and Colombo, G. (2006), "Human-centered robotics applied to gait training and assessment", *Journal of Rehabilitation Research and Development*, Vol. 43 No.5, pp. 679-694.

Saglia, J. A., Tsagarakis, N. G., Dai, J. S. and Caldwell, D. G. (2013), "Control Strategies for Patient-Assisted Training Using the Ankle Rehabilitation Robot (ARBOT)", *IEEE/ASME Transactions on Mechatronics*, Vol. 18 No.6, pp. 1799-1808.

Song, R., Tong, K.-y., Hu, X., and Li, L. (2008), "Assistive control system using continuous myoelectric signal in robot-aided arm training for patients after stroke", *IEEE Transactions on Neural Systems and Rehabilitation Engineering*, Vol. 16 No. 4, pp. 371-379.

Song, R., Tong, K. Y., Hu, X. L., and Zhou, W. (2013), "Myoelectrically controlled wrist robot for stroke rehabilitation", *Journal of Neuroengineering and Rehabilitation*, Vol. 10 No 25, pp.1-1.

Wolbrecht, E. T., Chan, V., Reinkensmeyer, D. J., and Bobrow, J. E. (2008), "Optimizing compliant, model-based robotic assistance to promote neurorehabilitation", *IEEE Transactions on Neural Systems and Rehabilitation Engineering*, Vol. 16 No. 3, pp. 286-297.

Xu, G. Z., Song, A. G. and Li, H. J. (2011), "Control System Design for an Upper-Limb Rehabilitation Robot", *Advanced Robotics*, Vol. 25 No.1-2, pp. 229-251.

Yin, Y. H., Fan, Y. J. and Xu, L. D. (2012), "EMG and EPP-Integrated Human-Machine Interface Between the Paralyzed and Rehabilitation Exoskeleton", *IEEE Transactions on Information Technology in Biomedicine*, Vol. 16 No.4, pp. 542-549.

Zhou, Z., Meng, W., Ai, Q. and et al. (2013), "Practical Velocity Tracking Control of a Parallel Robot Based on Fuzzy Adaptive Algorithm", *Advances in Mechanical Engineering*, Vol. 2013, Article ID 574896, 11 pages.